

# Bessel beam propagation: Energy localization and velocity

D. Mugnai\* and I. Mochi†

*Nello Carrara* Institute of Applied Physics-CNR,  
Via Panciatichi 64, 50127 Firenze, Italy

The propagation of a Bessel beam (or Bessel-X wave) is analyzed on the basis of a vectorial treatment. The electric and magnetic fields are obtained by considering a realistic situation able to generate that kind of scalar field. Specifically, we analyze the field due to a ring-shaped aperture over a metallic screen on which a linearly polarized plane wave impinges. On this basis, and in the far field approximation, we can obtain information about the propagation of energy flux and the velocity of the energy.

The motion of a Bessel beam is of great interest in physics both for its characteristic as a non-diffracting beam [1, 2, 3, 4, 5, 6, 7], and for its implications with regard to the topic of superluminality [8, 9, 10, 11, 12, 13]. Extended studies have been devoted to these subjects from both an experimental and a theoretical point of view. However, in spite of the many efforts devoted to this topic, no definite answer has been found about the amount of the energy transfer and its velocity.

As far as Bessel beam propagation is concerned, the problem is mainly related to the difficulty in finding the vectorial field that describes this system, while, on the contrary, the field in the scalar approximation is well-known.

The purpose of the present work is to investigate the propagation of a Bessel beam on the basis of a vectorial treatment. This kind of approach allows us to obtain information regarding the propagation of the energy flux and the energy mean velocity.

A Bessel beam consists of a set of plane waves with directions of propagation  $\mathbf{s} = \alpha_1 \mathbf{i} + \beta_1 \mathbf{j} + \gamma_1 \mathbf{k}$  which makes the same angle  $\theta_0$  ( $0 \leq \theta_0 < \pi/2$ ) with the  $z$ -axis (hence  $\gamma_1 = \cos \theta_0$  for all the plane waves). In spherical coordinates  $(\rho, \theta, \varphi)$ , the direction of propagation is specified by

$$\alpha_1 = \sin \theta_0 \cos \varphi, \quad \beta_1 = \sin \theta_0 \sin \varphi, \quad \gamma_1 = \cos \theta_0. \quad (1)$$

Thus, for propagation in vacuum or air, each one of these waves, at the point  $x, y, z$ , can be written as

$$u(P) = u_0 d\varphi \exp[ik_0(\alpha_1 x + \beta_1 y + \gamma_1 z)] \exp(-i\omega t), \quad (2)$$

where  $u_0 d\varphi$  is the amplitude of the elementary wave,  $\omega$  is the angular frequency,  $k_0 = \omega/c$  is the wavenumber, and  $x, y$  and  $z$  denotes the Cartesian coordinates of  $P$ . In cylindrical coordinates  $\rho, \psi, z$  around the  $z$ -axis

$$x = \rho \cos \psi, \quad y = \rho \sin \psi, \quad z \equiv z,$$

and the total field  $U$ , given by the superposition of all the waves (2), can be obtained by integrating over  $d\varphi$ , that is,

$$\begin{aligned} U &= u_0 \int_0^{2\pi} \exp[ik_0(\alpha_1 x + \beta_1 y + \gamma_1 z)] \exp(-i\omega t) d\varphi \\ &= 2\pi u_0 J_0(k_0 \rho \sin \theta_0) \exp\left(i\omega \frac{z}{c} \cos \theta_0\right) \exp(-i\omega t) \end{aligned} \quad (3)$$

where  $J_0$  denotes the zero-order Bessel function of first kind[14].

The scalar field of Eq. (3) is known as a Bessel beam (or Bessel-X wave), the unusual features of which are - that it does not change its shape during propagation, since its amplitude is independent of  $z$ [15];

---

\* E-mail: d.mugnai@ifac.cnr.it

† Permanent address: Osservatorio Astrofisico di Arcetri, L.go E. Fermi 5, 50125 Firenze, Italy

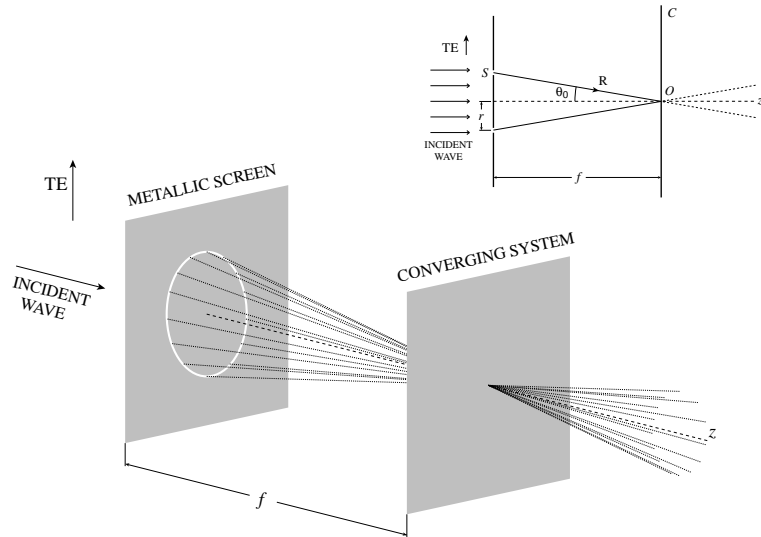


FIG. 1: Scheme of the system considered for the theoretical analysis presented here. The metallic screen (over which the ring-shaped aperture is placed) and the converging system must be considered as being of infinite dimension. Details are shown in the inset.

- that it propagates in the  $z$  direction with phase and group velocities  $v = c/\cos\theta_0$  larger than  $c$ [8, 9, 10, 16].

Both the above mentioned characteristics can be analyzed in detail by means of a vectorial treatment, since the scalar field (3) represents an approximation of an electromagnetic field, and only a knowledge of the vectorial field (and of the Poynting vector in particular) can provide detailed information about the energy propagation.

Vectorial fields with amplitude proportional to the zero-order Bessel function can be found in different ways. However, in order to derive just the vectorial field describing a system which has Eq. (3) as scalar approximation, we have to consider a realistic situation that is able to generate a field of that kind. For this purpose, let us consider the system of Fig. 1, which consists of a ring-shaped aperture, of radius  $r$ , over a metallic screen on which a linearly polarized plane wave impinges (from the left). The ring is placed on the focal plane of the converging system  $C$  with focal length  $f \gg \lambda$ ,  $\lambda$  being the wavelength. Let us consider the impinging electric field to be polarized in the  $\mathbf{i}$  direction, and the thickness  $d$  of the ring to be very small with respect to  $\lambda$ . We may assume the element  $dA$  of the ring, at  $S(r, \varphi, -f)$ , to behave as an elementary dipole, parallel to  $\mathbf{i}$ , with amplitude proportional to  $d\varphi$  (this requires a suitable choice of the transparency of the ring at  $S$ ). Thus, the associated field at the optical center  $O$  of  $C$  has the well-known characteristics of the far field radiated by an elementary dipole, that is to be a spherical wave centered at  $S$ , with the electric field  $\mathbf{e}$  in the meridional plane of the dipole through  $O$ , and perpendicular to the direction  $\mathbf{R}$  from  $S$  to  $O$ . We can write

$$\begin{aligned}\mathbf{R} &= -r \cos \varphi \mathbf{i} - r \sin \varphi \mathbf{j} + f \mathbf{k}, \\ \mathbf{e} &= e_x \mathbf{i} + e_y \mathbf{j} + e_z \mathbf{k}.\end{aligned}\quad (4)$$

The two characteristics mentioned above can be written as

$$\begin{aligned}\mathbf{e} \cdot \mathbf{R} &= -r \cos \varphi e_x - r \sin \varphi e_y + f e_z = 0 \\ (\mathbf{R} \times \mathbf{e}) \cdot \mathbf{i} &= f e_y + r \sin \varphi e_z = 0,\end{aligned}\quad (5)$$

where we disregarded a phase factor  $\exp(ikR)$ . By solving Eqs. (5) we obtain

$$e_y = -r \cos \varphi e_x \left( \frac{r \sin \varphi}{r^2 \sin^2 \varphi + f^2} \right) \quad (6)$$

$$e_z = r \cos \varphi e_x \left( \frac{f}{r^2 \sin^2 \varphi + f^2} \right). \quad (7)$$

At this point, we can assume that the field emerging from the optical converging system is a plane wave propagating in the direction of  $\mathbf{R}$ , with amplitude proportional to the amplitude at  $C$  of the incident field, namely [17]

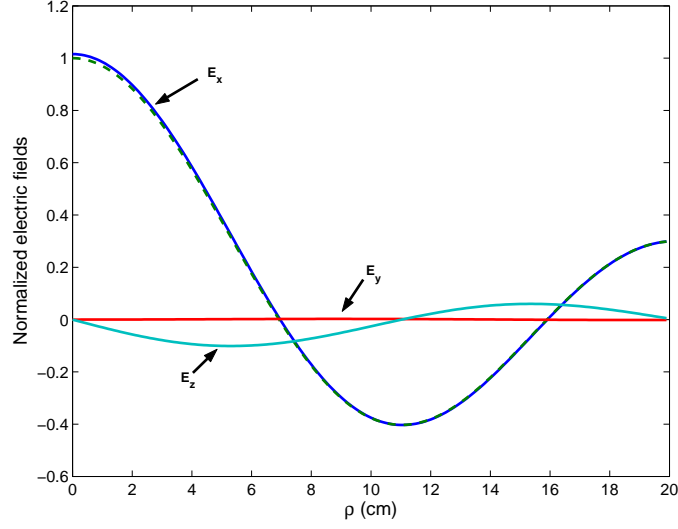


FIG. 2: Electric fields  $E_x$ ,  $E_y$  and  $E_z$  normalized to  $2\pi e_0 \exp(i\xi z)$  (continuous lines) vs.  $\rho$ , as given by Eqs. (12)-(14), for  $k = 2$ ,  $\psi = 10^\circ$  and  $\theta_0 = 10^\circ$ . In  $E_z$  phase factor  $e^{i\pi/2}$  is disregarded. The dashed line represents the normalized scalar field (3) for the same parameter values.

$$\mathbf{e} = (e_x \mathbf{i} + e_y \mathbf{j} + e_z \mathbf{k}) \exp[ik(\alpha x + \beta y + \gamma z)] \quad (8)$$

$$\mathbf{h} = \frac{1}{Z} \left[ (\alpha \mathbf{i} + \beta \mathbf{j} + \gamma \mathbf{k}) \times (e_x \mathbf{i} + e_y \mathbf{j} + e_z \mathbf{k}) \right] \exp[ik(\alpha x + \beta y + \gamma z)] \quad (9)$$

where  $\alpha = -\cos \varphi \sin \theta_0$ ,  $\beta = -\sin \varphi \sin \theta_0$ ,  $\gamma = \cos \theta_0$  are the director cosines,  $Z$  is the free-space impedance, and the temporal factor  $\exp(-i\omega t)$  is omitted. The total electric field  $\mathbf{E}$  will be given by the superposition of all  $e d\varphi$  contribution arising from the dipoles, and results in

$$\begin{aligned} \mathbf{E} &= \int_0^{2\pi} \mathbf{e} d\varphi = \int_0^{2\pi} (e_x \mathbf{i} + e_y \mathbf{j} + e_z \mathbf{k}) \exp \left\{ ik \left[ -\rho \left( \frac{r}{R} \right) \cos(\varphi - \psi) + \cos \theta_0 z \right] \right\} d\varphi \\ &= \exp(ik \cos \theta_0 z) \int_0^{2\pi} (e_x \mathbf{i} + e_y \mathbf{j} + e_z \mathbf{k}) \exp[-ik\rho \sin \theta_0 \cos(\varphi - \psi)] d\varphi. \end{aligned} \quad (10)$$

With reference to Eqs. (6) and (7), it is expedient to choose

$$e_x = \frac{e_0}{f^2} (r^2 \sin^2 \varphi + f^2) : \quad (11)$$

this condition can be experimentally obtained by a suitable choice of the transparency of the ring as a function of  $\varphi$ . Thus, by substituting Eqs. (6), (7) and (11) into Eq. (10), and by recalling that  $r = f \tan \theta_0$ , we finally obtain (calculations are rather cumbersome but of no difficulty)

$$E_x = 2\pi e_0 e^{i\xi z} \left\{ J_0(\eta\rho) + \tan^2 \theta_0 \left[ \left( J_0(\eta\rho) - \frac{J_1(\eta\rho)}{\eta\rho} \right) - \cos^2 \psi \left( J_0(\eta\rho) - \frac{2J_1(\eta\rho)}{\eta\rho} \right) \right] \right\} \quad (12)$$

$$E_y = -2\pi e_0 e^{i\xi z} \left[ \frac{\sin 2\psi}{2} \tan^2 \theta_0 \left( J_0(\eta\rho) - \frac{2J_1(\eta\rho)}{\eta\rho} \right) \right] \quad (13)$$

$$E_z = -2\pi i e_0 e^{i\xi z} [\tan \theta_0 \cos \psi J_1(\eta\rho)], \quad (14)$$

where  $\xi = k \cos \theta_0$ ,  $\eta = k \sin \theta_0$ , and  $J_1$  denotes the first-order Bessel function of first kind.

Equation (12) (the main contribution of the electric field) describes a field different from the scalar field of Eq. (3) because of the presence of the term depending on  $\tan \theta_0$ . However, for  $\theta_0 \ll \pi/2$  ( $r \ll f$ ), as in the present case, this

term is negligible. We note that also the dependence on  $\psi$  (which is absent in the scalar approximation) is negligible, and may be due to the approximation indicated in [17]. In Fig. 2 we report the normalized value of  $E_x$ ,  $E_y$  and  $E_z$  vs  $\rho$ , for  $\theta_0 = 10^\circ$ , together with the scalar field of Eq. (3). The scalar field is practically coincident with  $E_x$ . Therefore, we can conclude that the vectorial field derived above has Eq. (3) as its scalar approximation, at least for  $r \ll f$ .

The magnetic field can be derived by Eq. (9), and results in

$$H_x = 0 \quad (15)$$

$$H_y = \frac{2\pi}{Z} e_0 e^{i\xi z} \frac{1}{\cos \theta_0} J_0(\eta\rho) \quad (16)$$

$$H_z = -i \frac{2\pi}{Z} e_0 e^{i\xi z} \sin \psi \frac{\sin \theta_0}{\cos^2 \theta_0} J_1(\eta\rho) \quad (17)$$

From a knowledge of the electric and magnetic fields, we are now in a position to evaluate the mean density of the energy flux which is defined as one half of the real part of the complex Poynting vector[18, 19]

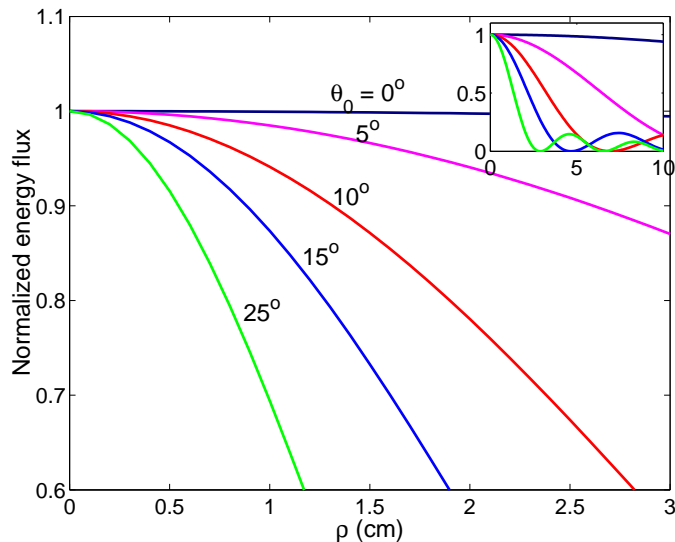


FIG. 3: Energy flux  $S_z$  as given by Eq. (19) normalized to its maximum value vs  $\rho$ , for a few values of  $\theta_0$ . For the sake of completeness, in the inset  $S_z$  is shown for larger values of  $\rho$ , even if only the region around the main peak is of physical interest. Parameter values are as in Fig. 2.

$$\mathbf{S} = \frac{1}{2} \text{Re}(\mathbf{E} \times \mathbf{H}^*). \quad (18)$$

For the fields (12)-(14) and (15)-(17), it turns out that  $S$  has only the  $k$ -component

$$S_z = \frac{1}{2} (E_x H_y^*), \quad (19)$$

that is the propagation of the energy flux occurs only in the  $z$ -direction, in accordance with the information given by the scalar field (3). Moreover, since the flux is independent of  $z$ , the energy propagates with no deformation.

In Fig. 3, the behavior of the energy flux (19) is shown as a function of  $\rho$  for a few values of  $\theta_0$ . We note that, for  $\theta_0$  very small (nearly plane wave) the flux is nearly independent of  $\rho$ , while when the beam originates the flux increases by increasing  $\theta_0$ , and tends to concentrate near  $\rho = 0$ , that is, along the  $z$ -axis. Thus, for small values of  $\rho$  (that is, in the proximity of the  $z$ -axis), the power supplied by a Bessel beam is always greater than the one due to a plane wave.

As for the velocity of the energy, from Eq. (3) it follows that in the scalar approximation the dependence of the field on  $t$  and  $z$  occurs only through the quantity  $(z/c) \cos \theta_0 - t$  and, therefore, the field propagates with velocity  $v = c/\cos \theta_0$ . On the basis of these arguments, it could be concluded that also the energy propagates with a velocity  $v_e$  greater than  $c$ . In the vectorial treatment we can evaluate the energy velocity  $v_e$  as [18, 19]

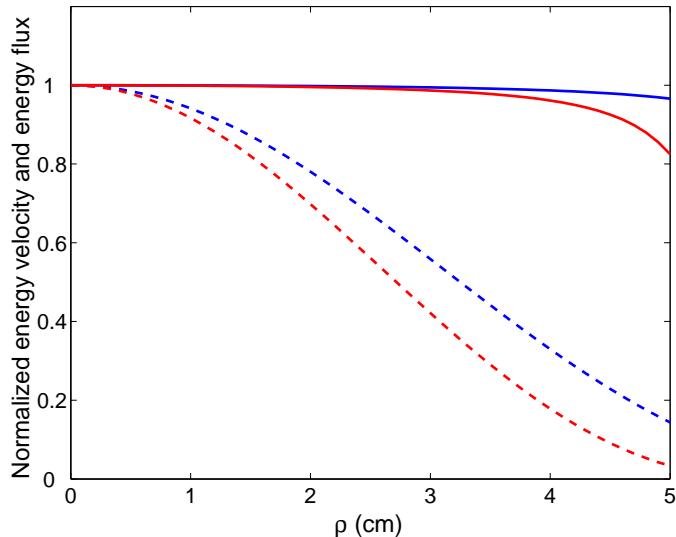


FIG. 4: Energy velocity normalized to the light velocity vs  $\rho$ , for  $k = 2$ ,  $\psi = 10^\circ$ ,  $\theta_0 = 10^\circ$  (blue line) and for  $\theta_0 = 12^\circ$  (red line). Dashed lines represent the energy flux relative to the same parameter values.

$$v_e = \frac{S_z}{\frac{1}{4}(\varepsilon E \cdot E^* + \mu H \cdot H^*)}, \quad (20)$$

where the quantity  $(1/4)(\varepsilon E \cdot E^* + \mu H \cdot H^*)$  is the total mean density of energy which can be evaluated with the help of Eqs. (12)-(14) and (15)-(17).

In Fig. 4, we report the normalized velocity of energy as a function of the radial coordinate  $\rho$ , for  $\theta_0 = 10^\circ$ . The velocity is found to be equal to  $c$  from  $\rho = 0$  up to near to the first zero of the Bessel function: that is, the beam moves like an almost rigid system, in spite of its dependence on  $\rho$  and  $\psi$ . In the proximity of the first zero of the Bessel function, the velocity decreases and tends to zero. Naturally, the zero in the velocity does not represent a stop of the motion but, more simply, the absence of energy flux. In this situation, the concept of velocity has no physical meaning.

Some remarks must be made on this surprising result. In fact, we recall that for propagation in vacuum “if an energy density is associated with the magnitude of the wave . . . . . the transport of energy occurs with the group velocity, since that is the rate of which the pulse travel along”[20]. If the definition of the energy velocity as given by Eq. (20) is applicable also to a Bessel beam (or, more generally, to localized waves), it is not clear what kind of physical mechanism makes the energy velocity different from the phase and group ones.

We wish to recall that the present analysis was performed for an ideal system in the far field approximation. For a real system, we have to take into account the finite dimension of the converging system, which limits the field depth and introduces diffractive effects. The role of diffraction, together with the analysis of the near field (as in real experimental situations), make the problem much more complicated, and is beyond the purpose of this paper.

### Acknowledgments

Special thanks are due to Laura Ronchi Abbozzo for useful suggestions and discussions.

- 
- [1] J. Durnin, J.J. Miceli Jr., and J.H. Eberly, Phys. Rev. Lett. **58**, 1499 (1987).
  - [2] J. Durnin, J. Opt. Soc. Am. A **4**, 651 (1987).
  - [3] Richard W. Ziolkowski, Phys. Rev. A **39**, 39 (1989).
  - [4] P. Sprangle and B. Hafizi, Phys. Rev. Lett. **66**, 837 (1991).
  - [5] J. Durnin, J.J. Miceli Jr., and J.H. Eberly, Phys. Rev. Lett. **66**, 838 (1991).

- [6] K. Tanaka, M. Taguchi, and T. Tanaka, *J. Opt. Soc. Am. A* **18**, 1644 (2001).
- [7] Kaido Reivelt and Peeter Saari, *Phys. Rev. E* **66**, 056611 (2002).
- [8] P. Saari and K. Reivelt, *Phys. Rev. Lett.* **79**, 4135 (1997).
- [9] D. Mugnai, A. Ranfagni, and R. Ruggeri, *Phys. Rev. Lett.* **84**, 4830 (2000).
- [10] I. Alexeev, K.Y. Kim, and H.M. Milchberg, *Phys. Rev. Lett.* **88**, 073901 (2002).
- [11] Ioannis M. Besieris and Amr M. Shaarawi, *Optics Express* **12**, 3848 (2004).
- [12] Miche Zamboni-Rached, Amr M. Shaarawi, and Erasmo Recami, *J. Opt. Soc. Am. A* **21**, 1564 (2004).
- [13] Peeter Saari and Kaido Reivelt, *Phys. Rev. E* **69**, 036612 (2004)
- [14] G.N. Watson, *Theory of Bessel Functions*, Cambridge, 1922.
- [15] The situation is similar to what occurs when only two plane waves interfere, the only difference being that the two-wave interference pattern occupies the whole space, while the field (3) is practically limited to a restricted zone of space, that is, to the first zero of the  $J_0$  function. In this connection, it is worth noting that the field of Eq. (3) is not properly a beam, since it is not limited by a caustic surface, inasmuch as  $J_0$  oscillates when its argument tends to infinity.
- [16] With respect to the monochromatic wave of Eq. (3), the situation does not change in the case of a wave packet (that is, for a modulated carrier). Also in this case, because of the absence of dispersion, all components at different frequencies do not suffer deformation and propagate with the same velocity.
- [17] To be precise, the amplitude of the field is not constant over a wavefront. We will neglect such a variation, which limits the applicability of our results to a small value of  $\theta_0$  and  $\rho$ . This position is justified also because we have to avoid the zeros of the field. In fact, when the field is zero, we lose information on the direction of propagation, and the Poynting vector may have some anomaly.
- [18] J. D. Jackson, *Classical Electrodynamics* (Wiley, New York,1999), Sec. 7.1.
- [19] J. A. Stratton, *Electromagnetic Theory* (McGraw-Hill, New York, 1941), p. 342
- [20] See Sec. 7.8 of Ref. [18].